J. Agric. Mach. Bioresour. Eng. 5(1&2), 2009 : 43-57 ISSN 1993-4041

Applications of Computational Fluid Dynamics (CFD) in Agriculture and Food Industry

B.K. Bala[1] and Tomoharu Yamaguchi[2]

Abstract

Applications of computational fluid (CFD) dynamics in agriculture and food industry are becoming important because of its versatility, accuracy and user friendliness. Now CFD is regularly used to solve environmental problems of structures and animal production systems. In the recent years this is becoming popular in drying and storage of agricultural products. This paper presents the state of art of CFD and its applications in greenhouse, animal housing, drying and storage. The potentials of CFD are also discussed.

Key words : Computational fluid dynamics, Heat and mass transfer, Green house, drying and storage

1. Introduction

Computational fluid dynamics, CFD, uses powerful computers and advanced numerical methods to model CFD problems and the success of the model is measured by the accuracy of predictions of the CFD models (Xia and Sun, 2002; Norton *et al.*, 2007). The advancement of powerful micro computers has paved the way for CFD and there has been a considerable development and growth of CFD in all aspects of fluid dynamics. Researchers are now increasingly using CFD to analyze and evaluate the problems of greenhouse, animal housing, drying and storage. In addition, CFD programs are considered powerful tool not only for fluid flow behaviour but also for drying and storage of agricultural products. Only recently CFD is being used in modeling of heat and mass transfer. CFD provides better understanding of the systems and, more over, softwares are now available to carry out the modeling of CFD even for complex systems. This paper presents the present state of art of CFD and its applications in greenhouse, animal housing, drying and storage.

2. Modeling of CFD

To predict velocity and temperature distribution inside greenhouses, cooling pad ventilated greenhouses and animal houses a set of equations consisting of continuity equation, energy balance equation and momentum balance equation are developed. For drying and storage of agricultural products in greenhouse, dryers, and storage, and cooling of agricultural products during storage, heat and mass transfer equations are included. The fundamentals of CFD modeling are given in Anderson (1995) and Versteeg and Malalasekera (1995). The fundamental equations to model the velocity and temperature distribution inside greenhouses, cooling pad ventilated greenhouses and animal houses are given below (Zhao *et al.*, 2006):

Continuity equation

$$\gamma_v \frac{\partial \rho}{\partial t} + \frac{\partial}{\partial x}(\gamma_x \rho u) + \frac{\partial}{\partial y}(\gamma_y \rho v) + \frac{\partial}{\partial z}(\gamma_z \rho w) = 0 \quad (1)$$

Momentum balance equation – x direction

$$\gamma_v \frac{\partial \rho u}{\partial t} + \frac{\partial}{\partial x}(\gamma_x u\, \rho u) + \frac{\partial}{\partial y}(\gamma_y v\, \rho u) + \frac{\partial}{\partial z}(\gamma_z w \rho u) = -\gamma_v \frac{\partial P}{\partial x} - R_z + \gamma_v \rho g_z$$

[1] Department of Farm Power and Machinery, Bangladesh Agricultural University, Mymensingh-2202, Bangladesh
e-mail: bkbalabau@yahoo.com
[2] Lab. of Bio-Environment Control Engineering, Doctoral Program in Bio-Industrial Sciences, Graduate School of Life and Environmental Sciences, University of Tsukuba, Japan
e-mail: yamatomo@agbi.tsukuba.ac.jp

$$+\gamma_v \rho b_x + \frac{\partial}{\partial x}\left(\gamma_x \mu_e 2\frac{\partial u}{\partial x}\right) + \frac{\partial}{\partial y}\left\{\gamma_y \mu_e\left(\frac{\partial u}{\partial y}+\frac{\partial v}{\partial x}\right)\right\} + \frac{\partial}{\partial z}\left\{\gamma_z \mu_e\left(\frac{\partial u}{\partial z}+\frac{\partial w}{\partial x}\right)\right\} \quad (2)$$

Momentum balance equation – y direction

$$\gamma_v \frac{\partial \rho v}{\partial t} + \frac{\partial}{\partial x}(\gamma_z u\, \rho v) + \frac{\partial}{\partial y}(\gamma_y v\, \rho v) + \frac{\partial}{\partial z}(\gamma_z w \rho v) = -\gamma_v \frac{\partial P}{\partial y} - R_y + \gamma_v \rho g_y$$

$$+\gamma_v \rho b_y + \frac{\partial}{\partial x}\left\{\gamma_x \mu_e\left(\frac{\partial v}{\partial x}+\frac{\partial u}{\partial y}\right)\right\} + \frac{\partial}{\partial y}\left(\gamma_x \mu_e 2\frac{\partial v}{\partial y}\right) + \frac{\partial}{\partial z}\left\{\gamma_z \mu_e\left(\frac{\partial v}{\partial x}+\frac{\partial u}{\partial y}\right)\right\} \quad (3)$$

Momentum balance equation – z direction

$$\gamma_v \frac{\partial \rho w}{\partial t} + \frac{\partial}{\partial x}(\gamma_z u\, \rho w) + \frac{\partial}{\partial y}(\gamma_y v\, \rho w) + \frac{\partial}{\partial z}(\gamma_z w \rho w) = -\gamma_v \frac{\partial P}{\partial z} - R_z + \gamma_v \rho g_z$$

$$+\gamma_v \rho b_z + \frac{\partial}{\partial x}\left\{\gamma_x \mu_e\left(\frac{\partial w}{\partial x}+\frac{\partial u}{\partial z}\right)\right\} + \frac{\partial}{\partial y}\left\{\gamma_y \mu_e\left(\frac{\partial w}{\partial y}+\frac{\partial v}{\partial z}\right)\right\} + \frac{\partial}{\partial z}\left(\gamma_z \mu_e 2\frac{\partial w}{\partial z}\right) \quad (4)$$

Energy balance equation

$$\gamma_v \frac{\partial \rho h}{\partial t} + \frac{\partial}{\partial x}(\gamma_z\, \rho u h) + \frac{\partial}{\partial y}(\gamma_y\, \rho v h) + \frac{\partial}{\partial z}(\gamma_z \rho w h)$$

$$= \gamma_v \frac{\partial P}{\partial t} + \frac{\partial}{\partial x}\left\{\gamma_x \lambda_e \frac{\partial T}{\partial x}\right\} + \frac{\partial}{\partial y}\left\{\gamma_y \lambda_e \frac{\partial T}{\partial y}\right\} + \frac{\partial}{\partial z}\left\{\gamma_z \lambda_e \frac{\partial T}{\partial z}\right\} + Q \quad (5)$$

Turbulent k – ε models

$$\gamma_v \frac{\partial \rho k}{\partial t} + \frac{\partial}{\partial x}(\gamma_z\, \rho u k) + \frac{\partial}{\partial y}(\gamma_y\, \rho v k) + \frac{\partial}{\partial z}(\gamma_z \rho w k) = \frac{\partial}{\partial x}\left\{\gamma_x\left(\mu + \frac{\mu_t}{\sigma_k}\right)\frac{\partial k}{\partial x}\right\}$$

$$+\frac{\partial}{\partial y}\left\{\gamma_y\left(\mu + \frac{\mu_t}{\sigma_k}\right)\frac{\partial k}{\partial y}\right\} + \frac{\partial}{\partial z}\left\{\gamma_z\left(\mu + \frac{\mu_t}{\sigma_k}\right)\frac{\partial k}{\partial z}\right\} + \gamma_v(G_s - \rho\varepsilon) \quad (6)$$

$$\gamma_v \frac{\partial \rho \varepsilon}{\partial t} + \frac{\partial}{\partial x}(\gamma_x\, \rho u \varepsilon) + \frac{\partial}{\partial y}(\gamma_y\, \rho v \varepsilon) + \frac{\partial}{\partial z}(\gamma_z \rho w \varepsilon) = \frac{\partial}{\partial x}\left\{\gamma_x\left(\mu + \frac{\mu_t}{\sigma_k}\right)\frac{\partial \varepsilon}{\partial x}\right\} +$$

$$\frac{\partial}{\partial y}\left\{\gamma_x\left(\mu + \frac{\mu_t}{\sigma_k}\right)\frac{\partial \varepsilon}{\partial y}\right\} + \frac{\partial}{\partial z}\left\{\gamma_z\left(\mu + \frac{\mu_t}{\sigma_k}\right)\frac{\partial \varepsilon}{\partial z}\right\} + \gamma_v\left\{C_1 \frac{\varepsilon}{k}(G_s + G_T)(1 + C_3 R_t) - C_2 \frac{\rho \varepsilon^2}{k}\right\} \quad (7)$$

$$G_s = \mu\left[2\left\{\left(\frac{\partial u}{\partial x}\right)^2 + \left(\frac{\partial v}{\partial y}\right)^2 + \left(\frac{\partial w}{\partial z}\right)^2\right\} + \left(\frac{\partial u}{\partial y}+\frac{\partial v}{\partial x}\right)^2 + \left(\frac{\partial v}{\partial z}+\frac{\partial w}{\partial y}\right)^2 + \left(\frac{\partial w}{\partial x}+\frac{\partial u}{\partial z}\right)^2\right] \quad (8)$$

$$G_T = \frac{\nu_t}{\sigma_t}\left(g_x \frac{\partial \rho}{\partial x} + g_y \frac{\partial \rho}{\partial y} + g_z \frac{\partial \rho}{\partial z}\right) \quad (9)$$

$$R_t = -\frac{G_T}{(G_s + G_T)} \quad (10)$$

$$\mu_t = C_\mu \frac{k^2}{\varepsilon} \tag{11}$$

$$\varepsilon = C_\mu \frac{k^{3/2}}{l} \tag{12}$$

Volume porosity and surface permeability are defined by

$$\gamma_v = \frac{V_{flow}}{V_{flow} + V_{obst}} \tag{13}$$

$$\left.\begin{aligned} \gamma_x &= \frac{(S_{flow})_x}{(S_{flow} + S_{obst})_x} \\ \gamma_y &= \frac{(S_{flow})_y}{(S_{flow} + S_{obst})_y} \\ \gamma_z &= \frac{(S_{flow})_z}{(S_{flow} + S_{obst})_z} \end{aligned}\right\} \tag{14}$$

3. CFD Analysis

The first step to the CFD analysis is a statement of the problem and then to express it mathematically that is formulation of the model. Then the CFD software package is used to expresses the stated problem in scientific terms. Finally, the computer is used to compute the dictated calculations by CFD software and the researcher should check and interpret the results. In principle, three different major steps should be undertaken for a CFD simulation (Shaw, 1992).

3.1. Pre-processing

All the tasks that are to be undertaken before the numerical solution using computer are called pre-processing. This includes mental model based on the statement of the problem, mesh generation and development of a computational model. Mental modelling is the first stage in using CFD. Before starting mathematical modeling, the physics of the problem should be clearly understood. The second stage is generation of the mesh. At this stage the researcher should generate the shape of the problem domain that needs to be analyzed. Next, the problem domain is sub-divided into numerous cells, also known as volumes and elements. Most of the CFD packages have programs to generate mesh and define the shape simultaneously. Once mesh generation is complete, the boundaries of the problem domain should be defined and the necessary boundary conditions, determined at the initial stage, should be applied. These conditions together with some fluid parameters and physical properties are used to specify the actual flow problem to be solved. Advanced CFD software packages have the program to carry out the following operations: defining a grid of points, also volumes or elements, defining the boundaries of the geometry, applying the boundary conditions, specifying the initial conditions, setting the fluid properties and setting the numerical control parameters. However, it is not easy to generate a complicated mesh.

3.2. Processing

Processing involves using a computer to solve mathematical equations of fluid flow. Once the meshing is completed, the model input values should be specified and then the software can be used to solve the equations of state for each cell until an acceptable convergence is achieved. This is a very intensive process and usually it requires the computer to solve many thousands of equations. In each case, the equations are integrated and the boundary conditions are applied to it. This is known as equation discretization and is applied to each individual cell of the mesh. The process is repeated in an iterative manner until a required accuracy is achieved. This step can be a time-consuming process and although it is the core of any CFD software package, little of its operation can be seen.

Standard softwares are now available for modeling using CFD. Fluent is one of the world's largest providers of commercial CFD softwares. It offers FLUENT, FIDAP and POLYFLOW (for polymer process) codes for a wide range of industrial applications. There are many researchers using FLUENT software. As the first step in building and analyzing a flow model, pre-processing is performed in two tools of FLUENT, GAMBIT and TGRID. FLUENT provides a wide array of advanced physical models for turbulence, combustion, and multiphase applications.

3.3. Post-processing

The post-processing program is to evaluate the data generated by the CFD analysis. When the model has been run using CFD, the results can be analyzed both numerically and graphically. Post-processing tools of the powerful CFD

software can create visualization ranging from simple 2-D graphs to 3-D representations. Typical graphs obtained with the post-processor might contain a section of the mesh together with vector plots of the velocity field or contour plots of scalar variables such as pressure. In such graphs, colours are used to differentiate between the different sizes of the values. When some results have been obtained, they must be analyzed, first to check whether the solution is satisfactory and then to determine the actual flow data that is required from the simulation.

4. APPLICATIONS

4.1. Greenhouse

Over much of the year, ventilation is required to guarantee an optimum greenhouse climate by promoting air exchanges between the air on the inside and the outside of the greenhouse. It thus maintains sound environmental conditions for plants by preventing excessive temperature build-ups around the plants during periods of strong solar radiation and by keeping relative humidity and carbon dioxide (CO_2) concentration at acceptable levels. Greenhouse ventilation may be natural, caused by wind and buoyancy forces, or mechanical, by using fans. Increased emphasis is being placed on natural ventilation at this time, which is the most energy efficient method and which provides the most uniform conditions. Natural ventilation is normally achieved by air exchanges through controlled lateral and/or roof openings. It largely depends on actors such as wind characteristics, air temperature differences between the inside and outside, and greenhouse design, as well as the presence of cultivated plants. Hence, managing the greenhouse climate by means of natural ventilation involves such a large number of parameters that it provides enduring challenges to researchers and is the reason why the prediction of air flux exchanges and mixing is still highly uncertain today. In particular, some questions still remain unanswered such as which strategy to adopt to properly design natural ventilation for maintaining sufficient circulation and good heat and mass transfer between plants and air.

Recent progress in flow modeling using computational fluid dynamics (CFD) provide a new opportunity to analyze the heterogeneity of the climate and to predict the ventilation rates in greenhouses. The CFD approach may provide a better understanding of the ventilation process for a wide range of greenhouse shapes, vent combination and boundary conditions and can help engineers and greenhouse manufacturers to improve greenhouse control and design.

Reichrath and Davies (2002) reported a comprehensive review of the state of art in the application of CFD in greenhouses. The first published work in this area by Okushima *et al.* (1989) was a small glasshouse with simple boundary conditions and the subsequent published work was more complex and realistic. The most realistic modeling study of a multi-span greenhouse has been carried out by Fatnassi *et al.* (2006). Their model was similar to Boulard and Wang (2002) and Roy and Boulard (2005) in that the transpiration phenomena of the indoor crop canopy were simulated as close to the physical situation as possible. Zhao *et al* (2006) developed a CFD model for a cooling pad ventilated greenhouse to predict air velocity and temperature distribution inside the greenhouse. Fig. 1 shows the predicted air velocity and temperature inside the greenhouse for different times during operation. The CFD predictions showed good agreement with experimental data. This indicates that CFD is a useful tool in the study of greenhouses.

4.2. Animal houses

Similar to the application of CFD in greenhouse design, many of the past animal housing studies lacked realism through the employment of broad assumptions and/or substandard modeling of the housing conditions. Only in recent times CFD has been used to model heat and mass transfer in a geometrical representation of an animal production facility (van Wagenberg *et al.*, 2004). The need for a dynamic representation of heat and mass transfer in livestock buildings in CFD studies has lately been acknowledged (Aerts and Berckmans, 2004; Gebremedhin and Wu, 2003). When dynamic models were used in conjunction with CFD predictions, they provided a more detailed picture of all the occurring phenomena (Gebremedhin and Wu, 2005). Because dynamic interactions have only recently been investigated, the accuracy afforded by CFD simulations has yet to be brought to the level at which greenhouse technology is currently situated.

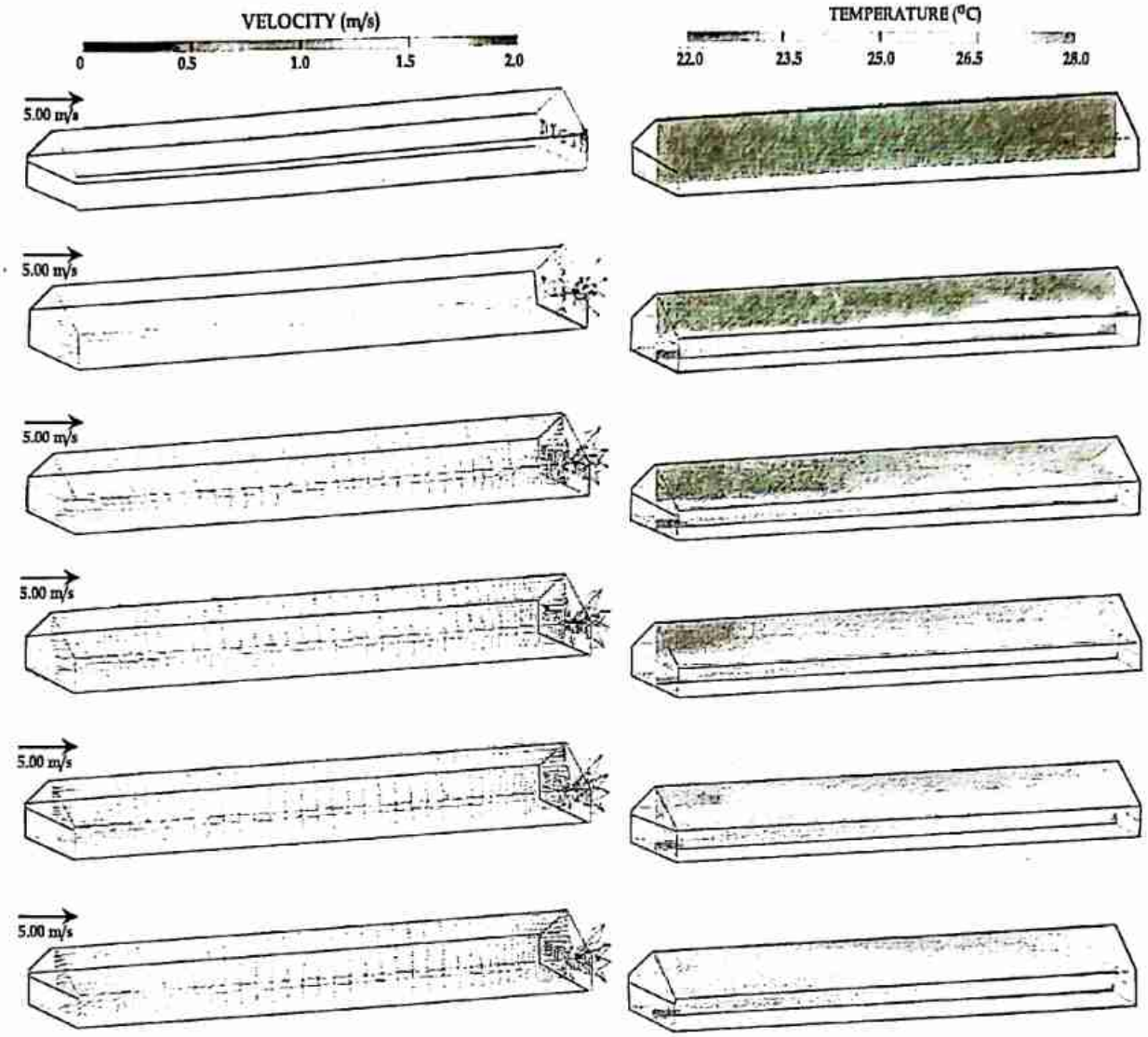

Fig. 1a. The predicted air velocity inside the greenhouse for different times (0, 120, 240, 360, 480 and 600 sec) starting from top during operation (Zhao *et al.*, 2006).

Fig. 1b. The predicted temperature inside the greenhouse for different times (0, 120, 240, 360, 480 and 600 sec) starting from top during operation (Zhao *et al.*, 2006).

4.2.1. Poultry houses

The indoor environment of poultry houses plays a decisive role in the ultimate success of a poultry industry. Air temperature, relative humidity, pollution concentration, thermal radiation and air movement directly affect the birds' ability to maintain homeothermy. If subjected to conditions outside the comfort zone, a bird needs to make physiological adjustments to maintain core body temperature (Tinoˆco *et al.*, 2001). This reduces production performance because dietary energy is used to produce or dissipate heat instead of being used for growth and development. Therefore, the requirement to keep the thermal environment within an optimal production range is evident. Yet, limited three CFD studies exist, in which the indoor environment of a poultry house has been investigated.

Due to numerical modeling constraints and small computational capacity, van Ouwerkerk *et al.* (1994) were only able to model two-dimensional air motion and heat transfer and, considering the associated limitations, aptly used the simulation results to determine locations within the building where environmental control sensors may act effectively. Mistriotis *et al.* (1997) studied the natural ventilation in a broiler house with a two-dimensional CFD model. The study focused on addressing the problem of meeting adequate

levels of ventilation on days of high solar radiation coupled with low wind speeds. The animals were modeled as a constant heat flux, which was represented by a heated floor. Mistriotis *et al.* (1997) found that by employing a solar chimney instead of conventional housing techniques, the indoor temperature and air velocity were maintained within the animals comfort zone. Both of the above studies highlighted the scope for the numerical simulation to aid in the better designing of housing systems for poultry. Lee *et al.* (2007) applied CFD model to investigate the natural ventilation in a broiler house and the most accurate CFD results were obtained when using a RNG k-ε turbulence numerical model. The average error of CFD computed air velocity when using the RNG k-ε turbulence numerical models was -6.2%.

High temperature is a major limiting factor in poultry production in many tropical areas of the world. The problem becomes severe when high temperature is accompanied by high humidity. Reduction in feed intake, growth rate and mortality due to heat stress are the consequences when birds are exposed to high temperature and high humidity. The thermo-neutral temperature for chicken is 18-25 ºC, where the birds perform at their maximum capacity. To alleviate heat stress on lying flock, the adverse effect on their egg production resulting from the inability of birds to dissipate heat at high temperature, increased ventilation rate and the use of high density diets have been suggested as a partial remedies. Enriched protein, amino acids, energy diets and supplements with electrolytes, and vitamins are commonly used in order to alleviate the effects of high temperature in poultry. However, these approaches are not quite enough to overcome the reduced performance in hot summer months. Increased ventilation and cooling the houses are the best approaches to alleviate heat problems. The genetic potentiality of the birds can express only in a comfortable housing environment. So, good housing environment is the prerequisite to have satisfactory growth and egg production from the flock.

Blanes-Vidal *et al.* (2008) developed four CFD simulations of airflows inside a mechanically ventilated commercial poultry building, by using different boundary conditions (corresponding to a single experimental scenario), and validated the CFD simulations by comparing the simulated and measured air velocities. The different comparisons carried out between measured and simulated air velocities showed that the simulations provide reasonable predictions of the velocities in the commercial poultry building (Fig. 2). The best fit between the CFD simulations and the experimental data was obtained when 'air velocity' at the inlets and 'percentage of airflow' at the outlets, both of which were calculated from the measured ventilation flow, were used as boundary conditions. Adjusting the CFD results by using at least 15 indoor air velocity measurements led to a more precise estimate of the mean air velocity at height of the birds. Air velocity at the height of the birds was 0.36±0.14 m/s obtained from measurements, 0.54±0.22 m/s obtained from the CFD simulations and 0.33±0.13 m/s from the adjustment of the CFD simulation results using 27 indoor air velocity measurements.

4.2.2. Cow houses

Only a few cases of CFD applications in cow housing are evident in the literature. Nonetheless, because the CFD simulations were used in conjunction with animal biological responses to determine the thermal environment, these studies have proved highly valuable and have raised the bar for future simulations. Gebremedhin and Wu (2003, 2005) solved the flow around cows to investigate, with an external program, the heat and mass transfer phenomena in a forced ventilated enclosure of simple geometry. They found that the total heat loss from an animal is highly dependant on both the animals' position and orientation to the flow field. For example, a cow positioned very close to the inlet had a total heat loss of 710 W, whereas an animal positioned to the back of the room had a heat loss of 214 W. Furthermore, a wall inlet producing a ceiling air jet seemed to create the most uniform environmental conditions in the building and minimized the large differences in animal heat loss (Gebremedhin and Wu, 2005). Even though Gebremedhin and Wu (2003, 2005) calculated heat and mass transfer from the simulated cows, only isothermal conditions were simulated in the CFD model. Consequently, this study was suggested to be the first step towards the develcpment of a comprehensive non-isothermal CFD model, in which heat production by a biological entity will be included.

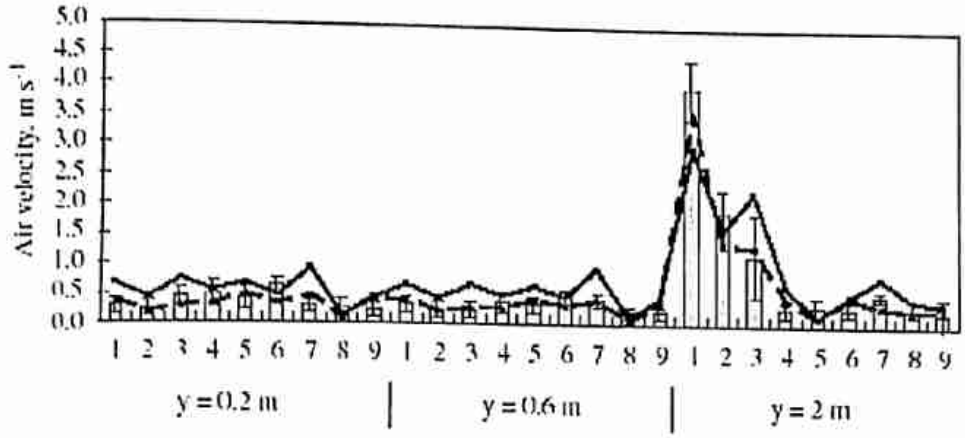

Fig. 2. Air velocities at 27 locations inside the poultry building: measured, CFD predicted adjusted. Error bars show standard deviations of the measurements (Blanes-Vidal *et al.*, 2008).

4.3. Drying

Drying of agricultural products such as fruits and vegetables in the tropics and subtropics is usually performed by traditional method of sun drying (Bala, 1998). This method is low cost, but the quality of the dried product is not up to mark of international standard. A method of increasing importance is forced convection dryer to dry products within few hours. The drying rate is a function of air flow rate or air velocity. Then it is important to know the air velocity in the drying chamber in order to know the areas of adequate or inadequate areas of air velocity. Computational fluid dynamics (CFD) may be used to predict the air velocity in the drying chamber. The simulation results of CFD may be tested against the experimental data and also can be used as a drying optimization tool.

Mathioulakis *et al.* (1998) simulated the drying of fruits in an industrial batch-type tray air dryer using CFD. The pressure profiles and the air velocity in the drying chamber were determined by CFD. Verboven *et al.* (2003) reported a CFD model to compute the air flow distribution in flatbed rice dryers in order to improve the dryers, which have been used for drying rice in Mekong Delta, Vietnam.

In the recent years, spouted bed drier has been developed to improve the productivity of the industrial drying process. Precise prediction of the flow field as well as the temperature and species distribution inside the bed is not possible using classical methods because the complex interactions between the gas and particles, but such predictions are important in the process design and scale up, and computational fluid dynamics can be used. By including heat and mass transfer within CFD simulations one can achieve the distributions of temperature and species .mass transfer. Szafran and Kmiec (2004) developed a CFD model for description of heat and mass transfer during drying of grain in a spouted bed dryer with a draft tube. Simulated results show that the most intense heat transfer occurs in small zones below the draft tube, where the dense bed comes into contact with the hot dry air. The largest temperature gradient is in these zones, but throughout the column, the temperature distribution is nearly uniform.

Kaya *et al.* (2008) studied the external flow and temperature fields during drying of Hayward kiwi fruits using a commercial CFD package. From these fields, the local distributions of the surface convective heat transfer coefficients for the fruits were determined to predict the local convective mass transfer coefficients through the analogy between the thermal and concentration boundary layers (known as the Chilton–Colburn analogy). In addition, the time-dependent temperature and moisture distributions for different cases were obtained using the code developed to investigate heat and mass transfer aspects inside the fruits. Fig. 3 shows the measured and predicted temperature values at the center inside the material with time and the predicted and measured values of the temperature at the center agree reasonably well. Fig. 4 shows the comparison between the predicted and measured moisture distributions at the center and a satisfactory agreement is also observed again.

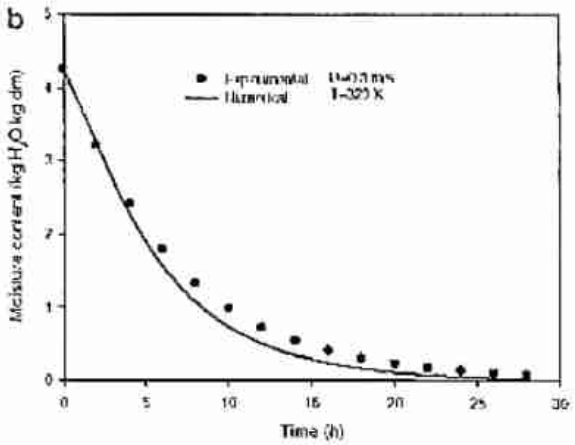

Fig. 3. Comparison between the calculated and measured center temperature distributions in the rectangular kiwi fruits (Kaya *et al.*, 2008).

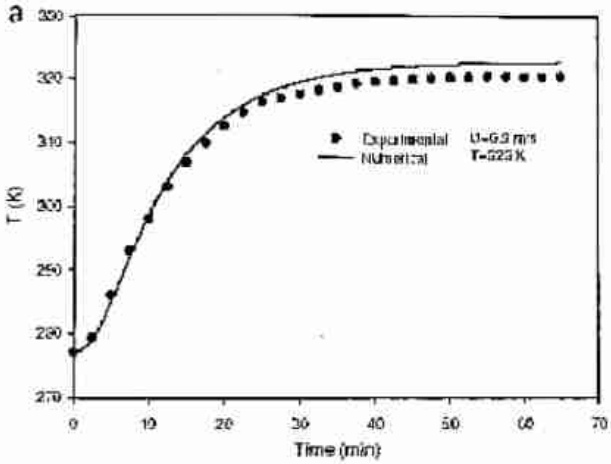

Fig. 4. Comparison between the calculated and measured center dimensionless moisture distributions in the rectangular kiwi fruits (Kaya *et al.*, 2008).

More recently Vijayaraj and Saravanan (2008) reported a CFD model using finite volume method to predict the temperature and moisture distribution of the moist rectangular baggase undergoing drying. The flow fields were predicted using FLUENT. Also the temperature and moisture distributions were obtained inside the material. Fig. 5 shows the temperature and moisture profile predicted by the model at various drying time (30, 300 and 600 s) for a bed thickness of 0.04m and drying air conditions at 100 ºC and 1 m/s. From the temperature profiles obtained for different times it is noticed that the temperature reaches almost steady-state within a few minutes from the time drying commenced, which is due to the effect of combined heat addition to the product by conduction from the bottom and by convection from the top surface. From the moisture profile contours in Fig. 5, the propagation of drying front within the product with time can be seen. It can be observed from the profile that the growth of the drying front propagation reduces with time, which is due to the reduction of the concentration gradient between the product surface and the drying medium as drying proceeds.

4.4. Storage

Several studies have been reported on modeling of the transport phenomena in bulk stored agricultural produces during cooling and/or storage with the forced convection cooling (Huzayyin *et al.*, 1973; Beukema *et al.*, 1982; Holdredge and Wyse, 1982; Alvarez and Trystram, 1995; Becker and Fricke, 1997; Tashtoush, 2000). In all these cases a physical system with thorough circulation of air was considered. However, some studies have been reported on cooling of agricultural produce under natural convection but, in these, the container surfaces were considered impermeable (Beukema *et al.*, 1983; Stewart and Dona, 1988; Burns and Stewart, 1992; Singh *et al.*, 1993; Casada and Young, 1994; Khankari *et al.*, 1994; Van der Sman, 1997; Xu *et al.*, 2002). However, in the packed bag of agricultural produce, such as potato, onion, etc., the surfaces are truly permeable and also exchange the mass and momentum with the environment apart from heat. Due to the permeable boundaries, the heat and mass transfer within the bag are strongly affected by the flow characteristics especially during the transient cooling process. This strong coupling between heat, mass and momentum transfer within such heat and mass generating porous media requires sophisticated numerical analysis methods to accurately trap the features of transport phenomena.

The computational fluid dynamics (CFD) technique based on the finite volume approach is one of the versatile numerical methods to analyze the heat, mass and momentum transfer under complex situations, although it requires certain modifications to make it applicable for a particular situation (Tassou and Xiang, 1998). Therefore, CFD has been used successfully by many researchers to model the airflow and heat transfer in bulk stored agricultural produce (Tassou and Xiang, 1998; Xu and Burfoot 1999a, 1999b; Nahor *et al.*, 2005). Many CFD codes are also available commercially. Of the available commercial

codes, some are of general purpose codes such as CFX-4, Phoenix, Fidap and Fluent, offering solutions to a wide range of fluid flow as well as heat and mass transfer problems (Scott and Richardson, 1997).

Chourisia and Goswami (2006 a and b) developed a model for fluid flow and heat transfer in a packed bag of potato. The model developed was investigated using the commercial available CFD code such as Fluent v.6_1_18. The governing equations were solved using finite volume approach to obtain the velocity field and temperature profiles within the potato bag during the transient cooling and steady state.

The contour plots of rate of moisture loss, in % per hour in the vertical (YZ) and one of the horizontal planes (XY) at 5 h, are shown in Figs. 6-7. The rate of moisture loss after 5 h of cooling increased as the distances from the bottom and sides of the bag increased as shown in Fig.6. The maximum moisture loss occurred just below the top surface in the central zone of the bag in spite of the high specific humidity in this zone. However, the overall variation in specific humidity within the bag was not considerable. The high rate of moisture loss in central upper zone of the bag was also due to the accumulation of heat resulting in a rise in temperature in this zone, which decreased the relative humidity therein. The contour of the rate of moisture loss maintained symmetry about both the horizontal axes (X and Y) as shown in Fig. 7. The maximum moisture loss occurred at the centre of the bag. The contours in Fig. 7 were compressed near the side of the bag and were scattered towards the centre due to the trend of decreasing temperature and velocity gradients towards the centre of the bag.

More recently Thorpe (2008) reported the application of CFD to simulate heat and moisture transfer in stored grains. Fig. 8 depicts the temperature distribution within the grain bulk. A so-called dwell region forms in a bulk of aerated grain between the trailing edge of the temperature-transfer wave and the leading edge of the moisture-transfer wave. When grain is being cooled its moisture content in the dwell region is somewhat lower than its initial moisture content, and the temperature is intermediate between that of the inlet air and initial temperature of the grain.

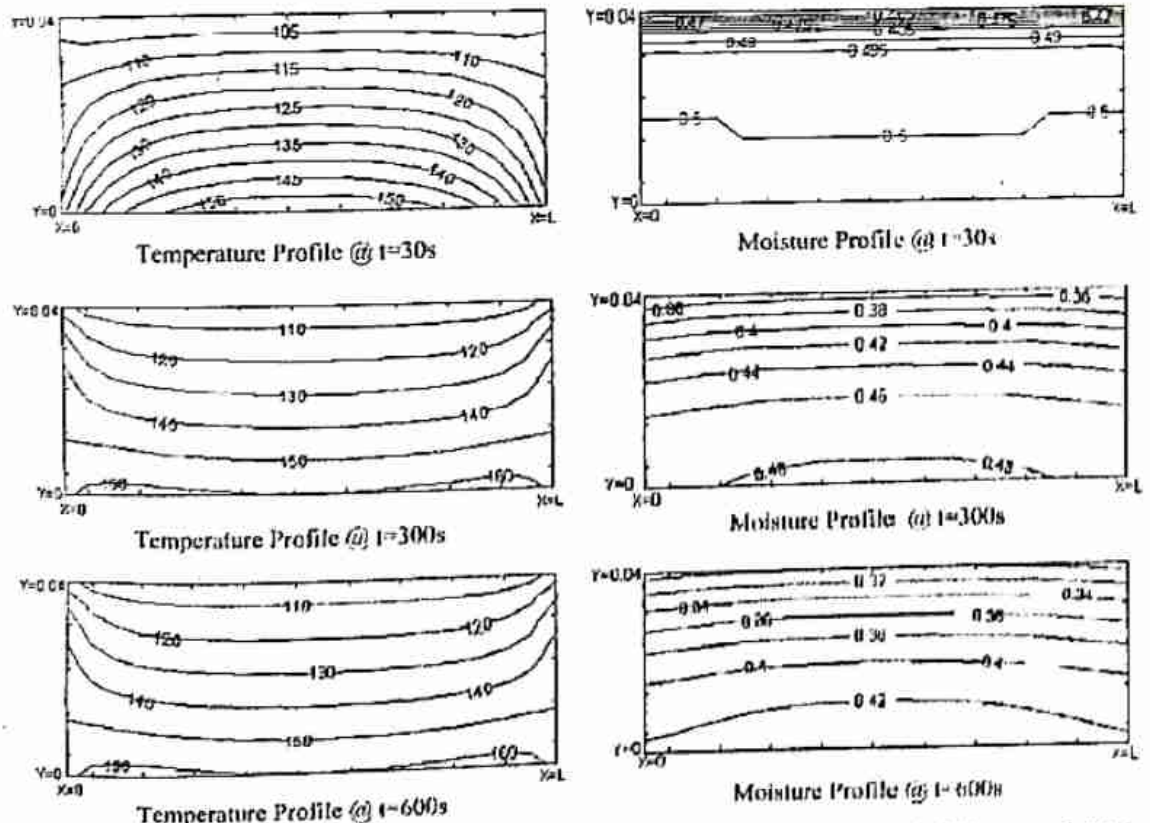

Fig. 5. Temperature and moisture profile predictions at various drying time for bed thickness of 0.04 m and conditions of air at 100°C and 1m/s. (Vijayaraj and Saravanan, 2008)

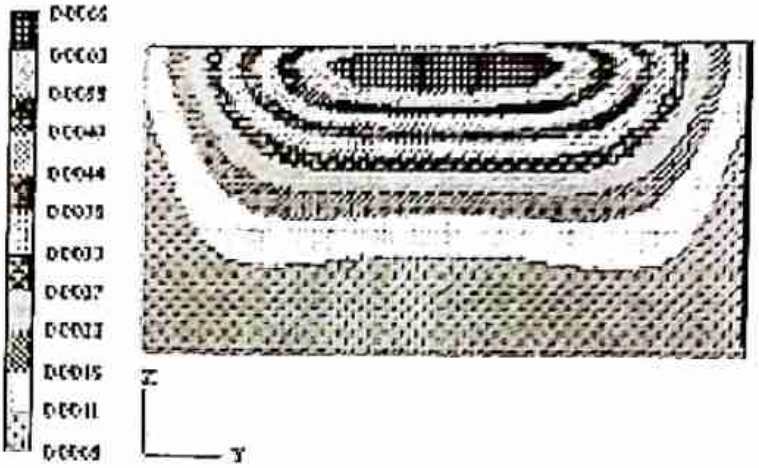

Fig. 6. Contours of rate of moisture loss in % [water] h^{-1} in the YZ plane inside the bag after 5 h of cooling (Chourisia and Goswami, 2006 a and b)

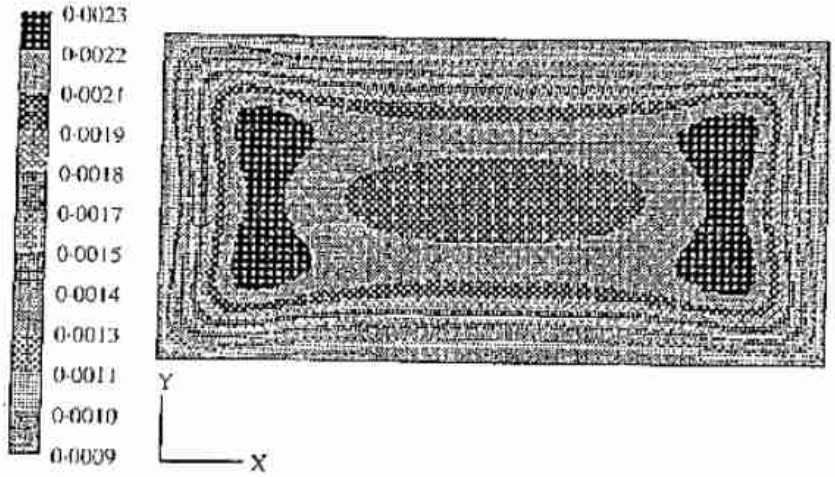

Fig. 7. Contours of rate of moisture loss in % [water] h^{-1} in the XY plane inside the bag after 5 h of cooling. (Chourisia and Goswami, 2006 a and b)

In Fig. 8 the red region represents grain that is yet to cool and it is still at 30ºC. The grain close to the air inlet on the left hand side of the bunker has cooled to 10ºC and it can be seen that a significant proportion of the grain is at the dwell temperature between 14 and 15ºC. A temperature transfer wave is apparent between the grain at the dwell temperature and the initial temperature, and the upper surface of the grain is at 30ºC. The moisture content of the grain reflects its temperature as indicated in Fig. 9. The region of grain not affected by the cooling temperature wave remains at its initial moisture content of 0.1346, and this falls to the dwell moisture content of about 0.13. Near the air inlet duct the grain moisture content rises to about 0.25 because it is approaching equilibrium with the high relative humidity air entering the grain.

4.5. Ventilated packaging

Forced-air cooling is the most common method for pre-cooling of horticultural produce to the optimum storage temperature. Ventilated packaging is required to achieve fast and uniform cooling. The cooling rates of produce mainly depend on heat transfer between cooling medium (air) and produce items in the packages. The heat transfer processes are closely related to airflow transport within the packages. Materials and configurations of produce packaging system have major impacts on the heat transfer and airflow patterns during force-air cooling. A packaging system needs to be carefully evaluated before implementation to ensure good cooling efficiency.

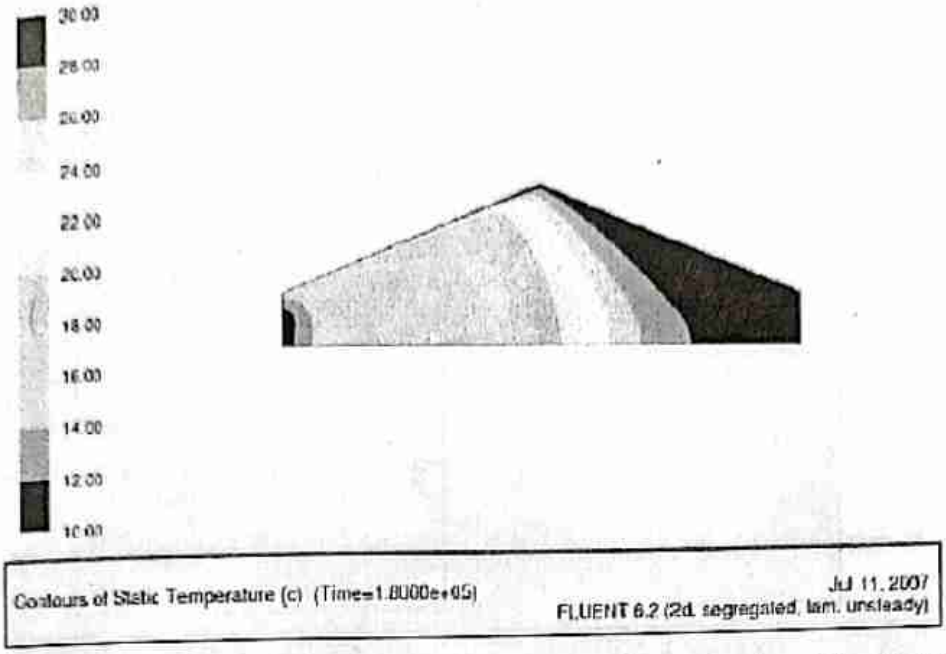

Fig. 8. Distribution of grain temperature in an aerated bulk of grain. The temperature of the dwell state is seen to be in the range 14–16°C. (Thorpe, 2008)

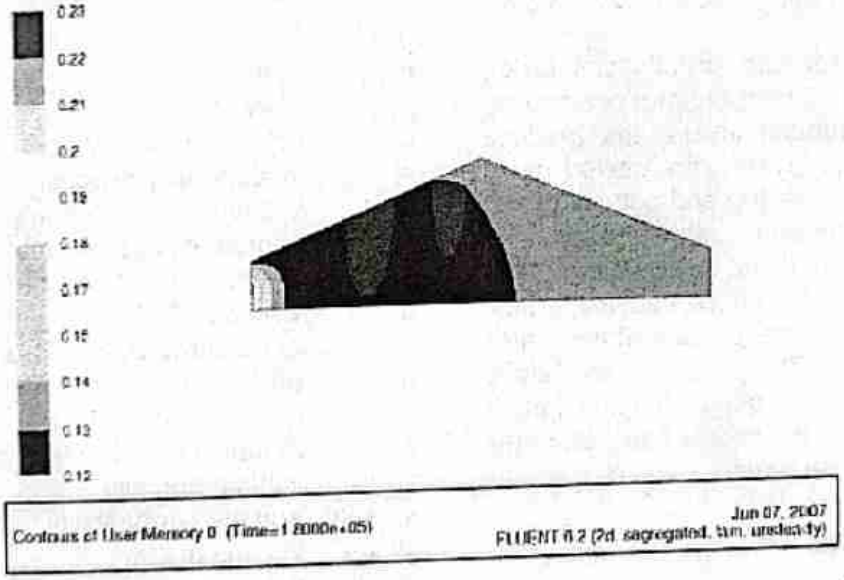

Fig. 9. Distribution of grain moisture content (fractional dry basis) in an aerated bulk of grain. The grain moisture content in the dwell region is in the range 0.12–0.13 fractional dry basis. (Thorpe, 2008)

Zou *et al.* (2006 a&b) developed a CFD model for simulating airflow and heat transfer processes to predict airflow patterns and temperature profiles in ventilated packaging systems during the forced-air cooling of fresh produce. Such a modeling system can find practical applications in evaluating forced-air cooling operations and assessing the cooling performance of alternative packaging designs for a range of horticultural commodities. CFD methods were used to solve the mathematical models for both layered and bulk packaging systems. Overall, the CFD modeling system gave satisfactory predictions of temperature profiles of fruit. When model predictions and experimental product center temperature data were compared, good agreements were obtained.

Fig. 10 shows the predicted air and produce temperature profiles of four produce layers after 1 h of forced-air cooling. The temperature profiles were expressed with collection of colours, and the meanings of these colours were explained with the colour bars on the figures. The coloured circular areas in cells

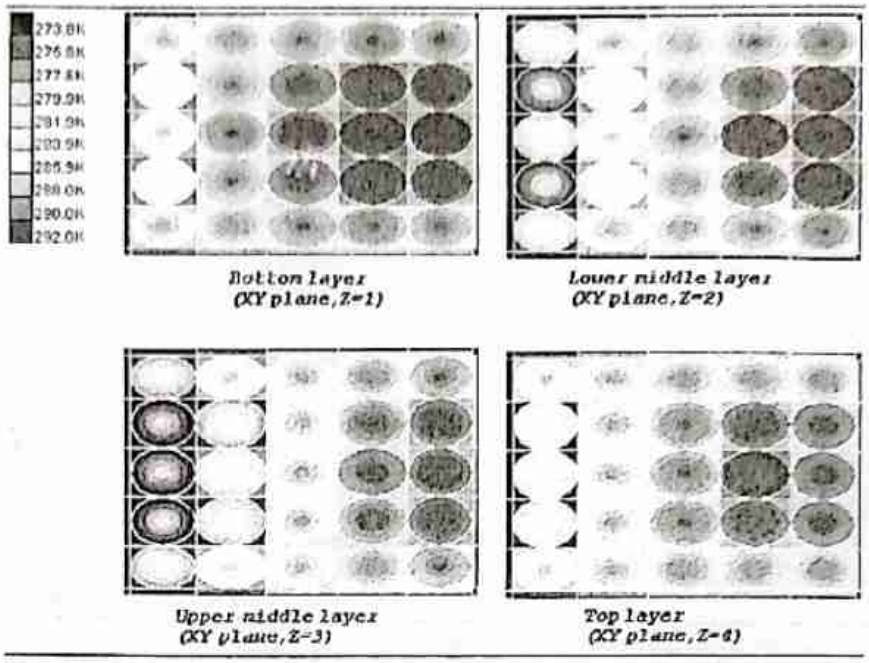

Fig. 10. Predicted air and produce temperature profiles in the produce layers of a single Z-Pack apple carton after 1 h of cooling (Zou *et al.*, 2006 a & b)

illustrate the temperature distributions inside produce items. Comparing the produce cooling rates in these produce layers, the produce items in the middle layers were cooled much faster than those in the top and bottom layers. This result was consistent with the distribution of cooling media (air) in these layers. The produce items near the inlets had the fastest cooling rates due to the biggest airflow rates around these items. The produce items along the package walls were generally cooled more rapidly than those in the middle because of the relatively large airflow rates.

5. Conclusions

This paper critically reviews the applications of CFD in agriculture and food industry. CFD can be used as a tool for prediction of performance and design of greenhouse environment, animal housing, drying, and storage systems. However, CFD simulated prediction should be validated by experiments.

Nomenclature

P	pressure Pa
Q	rate of work done by the body force kW/m^3
R	body force N/m^3
T	temperature °C
b	component acceleration m/s^2
g	gravitational acceleration m/s^2
h	enthalpy J
t	time s
u	velocity in x direction m/s
v	velocity in y direction m/s
w	velocity in z direction m/s
x, y, z	coordinate system m
υ	kinetic viscosity m^2/s
μ	viscosity Pa*s
μ_t	turbulent viscosity Pa*s
μ_e	effective turbulent viscosity Pa*s ($\mu_e = \mu_t + \mu$)
λ_e	thermal conductivity W/m-K
γ_v	volume porosity
γ_x γ_y γ_z	surface permeability
V_{flow}	volume of flow
V_{obst}	volume of obstruction
S_{flow}	surface perpendicular to flow
S_{obst}	surface perpendicular to obstruction
ρ	air density kg/m^3
k	turbulent kinetic energy m^2/s^2
ε	dissipation rate of turbulent kinetic energy m^2/s^3
ℓ	turbulent length m

References

Aerts J M and Berckmans D 2004. A virtual chicken for climate control design: static and dynamic simulations of heat losses. Transactions of the ASAE, 47(5), 1765–1772.

Alvarez G, and Trystram G 1995. Design of a new strategy for the control of the refrigeration process: fruits and vegetables conditioned in a pallet. Food Control, 6(6), 347–355.

Anderson Jr, J D 1995. Computational Fluid Dynamics: The Basics with Applications. Mc Graw Hill, New York.

Bala B K 1998. Solar Drying Systems: Simulation and Optimization. Agrotech Publishing Academy, Udaipur, India.

Becker B R and Fricke B A 1997. Modeling transport phenomena in heat and mass releasing porous media. International Communications in Heat and Mass Transfer, 24(3), 439–448.

Beukema K J, Bruin S and Schenk J 1982. Heat and mass transfer during cooling and storage of agricultural products. Chemical Engineering Science, 37(2), 291–298.

Beukema K J, Bruin S and Schenk J 1983. Three-dimensional natural convection in a confined porous medium with internal heat generation. International Journal of Heat and Mass Transfer, 26(3), 451–458.

Blanes-vidal V, Guijarro E, Balasch S and Torres A G 2008. Application of computational fluid dynamics to the prediction of airflow in a mechanically ventilated commercial poultry building. Biosystems engineering, 100(1),105–116.

Boulard T and Wang S 2002. Experimental and numerical studies on the heterogeneity of crop transpiration in a plastic tunnel. Computers and electronics in agriculture, 34(1-3), 173–190.

Burns A S and Stewart Jr, W E 1992. Convection in heat generating porous media in a concentric annulus with a permeable outer boundary. International Communications in Heat and Mass Transfer, 19, 127–136.

Casada M E and Young J H 1994. Model for heat and moisture transfer in arbitrarily shaped two-dimensional porous media. Transactions of the ASAE, 37(6), 1927–1938

Chourasia M K and Goswami T K 2006a. Simulation of transport phenomena during natural convection cooling of bagged potatoes in cold storage, Part II: Mass Transfer. Biosystems Engineering, 94(2), 207–219.

Chourasia M K and Goswami T K 2006b. Simulation of transport phenomena during natural convection cooling of bagged potatoes in cold storage, Part I: Fluid flow and heat transfer. Biosystems Engineering, 94(1), 33–45.

Fatnassi H, Boulard T, Poncet C and Chave M 2006. Optimization of greenhouse insect screening with computation fluid dynamics. Biosystems Engineering, 93, 301–312.

Gebremedhin K G and Wu B X 2003. Characterization of flow field in a ventilated space and simulation of heat exchange between cows and their environment. Journal of Thermal Biology 28, 301–319.

Gebremedhin K G and Wu B X 2005. Simulation of flow field of a ventilated and occupied animal space with different inlet and outlet conditions. Journal of Thermal Biology, 30, 343–353.

Holdredge T M and Wyse R E 1982. Computer simulation of forced convection cooling of sugarbeets. Transactions of the ASAE, 25, 1425–1430.

Huzayyin A S, Hodges T O and Miller P L 1973. Unsteady-state cooling of high moisture corn. Transactions of the ASAE, 16, 717–723.

Khankari K K, Morey R V and Patankar S V 1994. Mathematical model for moisture diffusion in stored grain due to temperature gradients. Transactions of the ASAE, 37(5), 1591–1604.

Kaya A, Aydyn O and Dincer I 2008. Experimental and numerical investigation of heat and mass transfer during drying of Hayward kiwi fruits (Actinidia Deliciosa Planch). Journal of Food engineering, 88, 323-330.

Lee I, Sase S and Sung S 2007. Evaluation of CFD accuracy for the ventilation study of a naturally ventilated broiler house. JARQ, 41(1), 53–64.

Mathioulakis E, Karathanos V T and Belessiotis V G 1998. Simulation of air movement in a dryer by computational fluid dynamics: Application for the drying of fruits. Journal of Food Engineering, 36, 183-200.

Mistriotis A, de Jong T, Wagemans M J M. and Bot G P A 1997. Computational fluid dynamics as a tool for the analysis of ventilation and indoor microclimate in agricultural buildings. Netherlands Journal of Agricultural Science, 45, 81–96.

Nahor H B, Hoang M L, Verboven P, Baelmans M and Nicolai B M 2005. CFD model of the airflow, heat and mass transfer in cool stores. International Journal of Refrigeration, 28, 368–380.

Norton T, Sun D, Grant Z, Fallon R and Dodd V 2007. Applications of computational fluid dynamics (CFD) in the modelling and design of ventilation systems in the agricultural industry: A review. Bioresource Technology, 98(12), 2386-2414.

Okushima L, Sase S and Nara M A 1989. A support system for natural ventilation design of greenhouses based computational acrodynamics. Acta Horticulturae, 284, 129–136.

Reichrath S and Davies T V 2002. Using CFD to model the natural internal climate of greenhouses: past, present and future. Agronomie, 22, 3–19.

Roy J C and Boulard T 2005. CFD prediction of the natural ventilation in a tunnel type greenhouse: Influence of wind direction and sensitivity to turbulence models. Acta Horticulturae, 691, 457–464.

Scott G and Richardson P 1997. The application of computational fluid dynamics in the food industry. Trends in Food Science and Technology, 8, 119–124.

Shaw C T 1992. Using Computational Fluid Dynamics. Prentice Hall, New Jersey, USA.

Singh A K, Leonardi E and Thorpe G R 1993. A solution procedure for the equations that govern three-dimensional free convection in bulk stored grains. Transactions of the ASAE, 36(4), 1159–1173.

Stewart Jr, W E and Dona C L G 1988. Numerical analysis of natural convection heat transfer in stored high moisture corn. Journal of Agricultural Engineering Research, 40, 275–284.

Szafran R G and Kmiec A 2004. CFD Modeling of heat and mass transfer in a spouted bed dryer. Ind. Eng. Chem. Res., 43, 1113-1124.

Tanner J D 1998. Mathematical modelling for design of horticultural packaging. PhD thesis, Massey University, Palmerston North, New Zealand.

Tashtoush B 2000. Heat-and-mass transfer analysis from vegetable and fruit products stored in cold conditions. Heat and Mass Transfer, 36, 217–221.

Tassou S A and Xiang W 1998. Modeling the environment within a wet air-cooled vegetable store. Journal of Food Engineering, 38, 169–187.

Tinoˆco I F F, Zanolla N, Alvarenga e Melo R C, Baeˆtal F C, Tinoˆco A L A, Yanagi Jr T, Moraes S R P and Silva J N 2001. Effect of different ventilation systems on hot weather thermal comfort and performance of broiler chickens raised at high placement. In: Livestock Environment VI: Proceedings of the 6th International Symposium, Louisville, Kentucky, USA. pp. 250–255.

Thorpe G R 2008. The application of computational fluid dynamics codes to simulate heat and moisture transfer in stored grains. Journal of Stored Products Research, 44, 21–31.

Van der Sman R G M 1997. Lattice Boltzmann scheme for natural convection in porous media. International Journal of Modern Physics, 8(4), 879–888.

van Ouwerkerk E N J, Voskamp J P and Aliskan Y 1994. Climate simulation and validation for an aviary system for laying hens. Institute of Agricultural and Environmental Engineering, Report N 94-C-063, AgENG, Milan, Italy.

van Wagenberg A V, Bjerg B and Bot G P A 2004. Measurements and simulation of climatic conditions in the animal occupied zone in a door ventilated room for piglets. Agricultural Engineering International: The CIGR Journal of Scientific Research and Development, Manuscript BC 03 020, Vol. VI.

Verboven P, Verboven P, Baelmans M, Baerdemaeker J and Nicolai B M 2003. Simulation of air flow in a flatbed dryer by computational fluid dynamics: Applications for drying rice in Mekong delta, Vietnam. ASAE paper Number 036229, 2003 annual meeting.

Versteeg H K and Malalasekera W 1995. An Introduction to Computational Fluid Dynamics. Prentice Hall, London.

Vijayaraj B and Saravanan R 2008. Numerical modeling of moisture and temperature distribution within a rectangular baggase layer undergoing drying. Drying Technology, 26, 749–758.

Xia B and Sun Da-Wen. 2002. Applications of computational fluid dynamics (CFD) in the food industry: A review. Computers and electronics in agriculture, 34, 5-24.

Xu Y and Burfoot D 1999a Simulating the bulk storage of foodstuffs. Journal of Food Engineering, 39, 23-29.

Xu Y and Burfoot D 1999b. Predicting condensation in bulks of foodstuffs. Journal of Food Engineering, 40, 121–127.

Xu S, Jayas D S, White N D G and Muir W E 2002. Momentum diffusive model for gas transfer in granular media. Journal of Stored Products Research, 38, 455–462.

Zhao S, Yamaguchi T, Hoshi N, Kuroyanagi T and Li B 2006. Analysis of air-movement and temperature distribution in the pad and fan cooling greenhouse by computational fluid dynamics. Journal of the Society of Agricultural Structures, 36(1), 17-26.

Zou Q, Opara L U and McKibbin R 2006b. A CFD modeling system for airflow and heat transfer in ventilated packaging for fresh foods: II. Computational solution, software development, and model testing. Journal of Food Engineering, 77(4), 1048-1056.

Zou Q Opara L U and McKibbin R 2006a. A CFD modeling system for airflow and heat transfer in ventilated packaging for fresh foods: I. Initial analysis and development of mathematical models. Journal of Food Engineering, 77(4), 1037-1047.